DUAL-BAND COMPOSITE RIGHT/LEFT-HANDED RING ANTENNA WITH LINEAR/CIRCULAR POLARIZATION CAPABILITY

A. Rennings [(1)], S. Otto [(1)], T. Liebig [(1)], C. Caloz [(2)], I. Wolff [(1)]

[(1)] IMST GmbH, Carl-Friedrich-Gauß-Str. 2, D-47475 Kamp-Lintfort, Germany, Email: A.Rennings@ieee.org
[(2)] École Polytechnique, 2500 ch. de Polytechnique, H3T 1J4 Montréal, Canada

ABSTRACT

A dual-band metal-insulator-metal (MIM) composite right/left-handed (CRLH) λ-resonance ring antenna with multi-polarization (linear/circular) radiation capability is demonstrated by way of full-wave simulations. The theory, design guidelines, parameter extraction procedure and feeding structure of this antenna are presented and discussed.

1. INTRODUCTION

The concept of CRLH transmission lines has been extensively applied to various novel types of microwave devices, including couplers, resonators and antennas [1]. The CRLH concept takes into account and exploits the dual nature of practical left-handed (LH) structures, which also include natural right-handed (RH) contributions.

A linearly-polarized dual-band CRLH λ-resonance ring antenna was presented in [2]. In this paper, we propose a dual-band CRLH λ-resonance ring antenna, which includes two additional aspects. Functionally, it is capable of *multi-polarization*, including linear and circular, in addition to dual-band operation. Technologically, it is implemented in the simpler, more compact and spurious-free *MIM CRLH technology* [3]. The combination of these two aspects leads to a highly versatile and cost-effective antenna solution for modern wireless communication systems (e.g. IEEE 802.11a,b,g).

2. THEORY AND DESIGN GUIDELINES

Fig. 1 shows the proposed CRLH TL ring configuration. Each unit cell, of azimuthal length or period p, is modelled by its equivalent lumped circuit shown in the inset of the figure. By applying *ABCD* matrix formalism and periodic boundary conditions to the unit cell's terminals, the propagation constant $\beta(\omega)$ (or dispersion relation) based on the four lumped element parameters L_R, C_L, L_L, C_R and the physical unit cell size p for an infinite transmission line is found as

$$\beta(\omega) = \pm\frac{1}{p}\mathrm{Re}\left\{\arccos\left(1-\frac{1}{2}\frac{\left(\omega^2-\omega_{sh}^2\right)\left(\omega^2-\omega_{se}^2\right)}{\left(\omega_R\omega\right)^2}\right)\right\} \quad (1)$$

with $\omega_{se} = 1/(C_L L_R)^{1/2}$, $\omega_{sh} = 1/(C_R L_L)^{1/2}$, $\omega_R = 1/(C_R L_R)^{1/2}$ and $\omega_L = 1/(C_L L_L)^{1/2}$.

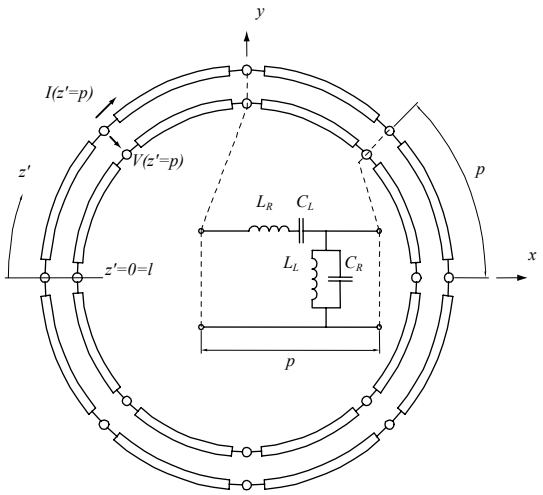

Figure 1. CRLH TL ring configuration composed of N = 8 cascaded unit cells. Each CRLH transmission line section is modelled with the lumped element equivalent circuit shown in the inset.

In the so-called *balanced* case, which is defined by $\omega_{se} = \omega_{sh} = \omega_0$ and which corresponds to a design with broadband matching, the function (1) can be inverted as

$$\omega(\beta) = \sqrt{\omega_0^2 + \omega_R^2 \sin^2\left(p\,\beta/2\right)} + \omega_R \sin\left(p\,\beta/2\right), \quad (2)$$

which may also be used as an approximation in the case a slightly unbalanced design. The following useful relation, relating the dispersion frequencies of the LH and RH waves with same guided wavelength, may be derived from Eq. (2)

$$\sqrt{\omega(-|\beta|)\,\omega(|\beta|)} = \omega_0. \quad (3)$$

The resonance condition for this configuration is that the circumference of the ring l should be a multiple of λ_g, as for a conventional ring resonator. If the ring is constituted of N unit cells, we have $l = Np = n\lambda_g$, where n is the (integer) mode index. The resonance frequencies ω_n can be determined with Eq. (2) as

$$\omega_n = \sqrt{\omega_0^2 + \omega_R^2 \sin^2(\pi n/N)} + \omega_R \sin(\pi n/N), \quad (4)$$

and Eq. (3) becomes

$$\sqrt{\omega_{-|n|}\ \omega_{+|n|}} = \sqrt{\omega_{-1}\ \omega_{+1}} = \omega_0. \quad (5)$$

In the case of a λ_g ($n = \pm 1, -1$ in LH band and +1 in RH band) dual-band resonator, Eq. (4) particularizes to

$$\omega_{-1,+1} = \sqrt{\omega_0^2 + \omega_R^2 \sin^2(\pi/N)} \mp \omega_R \sin(\pi/N). \quad (6)$$

From this relation, we have

$$N = \frac{\pi}{\arcsin\left(\dfrac{\omega_{+1} - \omega_{-1}}{2\ \omega_R}\right)}, \quad (7)$$

which determines the number of unit cells needed as function of the two operation frequencies and a given ω_R parameter corresponding to a given unit cell. It can be seen that the required number of cells decreases as the spacing between the two frequencies increases. The maximum spacing between the two frequencies is given by $(\omega_{+1} - \omega_{-1})/\omega_R < 2$. Fig. 2 shows relation (7).

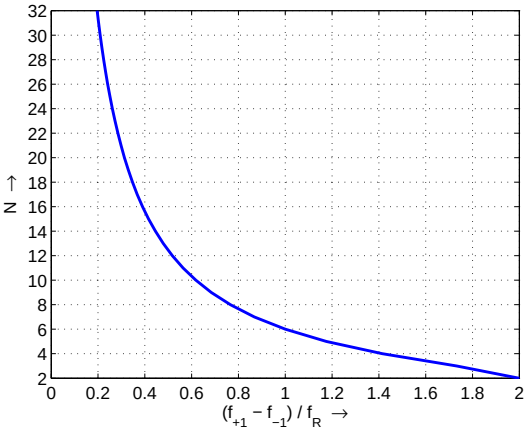

Figure 2. Plot of Eq. (7) giving the number of cells as a function of the difference between the two operation frequencies f_{+1} and f_{-1}.

Fig. 3 shows the dispersion diagram and resonances for a specific design.

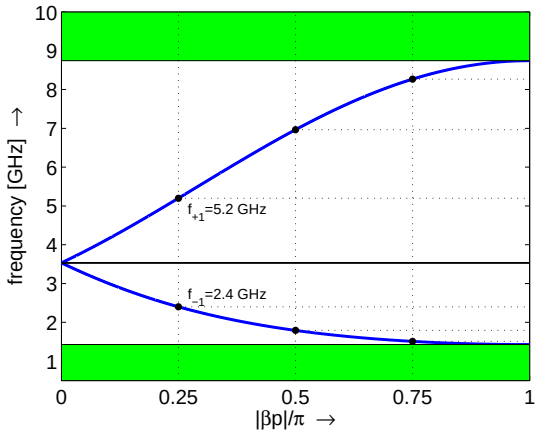

Figure 3. Dispersion diagram computed by Eq. (2) for the following specifications f_{-1} = 2.4 GHz and f_{+1} = 5.2 GHz and with the parameters C_R = 0.87pF, C_L = 0.93pF, L_R = 2.2nH and L_L = 2.3nH, which implies N=8 according to Eq. (7).

The design of the dual-band ring antenna consists in determining its 5 parameters L_R, C_R, L_L, C_L and N. The guidelines for an initial design are as follows:

1) determine the values of the L_L and C_L of the unit cell typically achievable in the technology to be used (extraction of lumped element values is explained in section 4), which fixes ω_L;
2) the layout configuration of the unit cell used for these LH elements will induce some RH parasitic values L_R and C_R, which fixes ω_R;
3) fine-tune the layout in order to meet the balanced condition $\omega_R\ \omega_L = \omega_0^2 = \omega_{-1}\ \omega_{+1}$.
4) determine the number of unit cells N by Eq. (7) for the two frequencies specified f_{+1} and f_{-1}.

3. MIM UNIT CELL IMPLEMENTATION

A CRLH structure can be most conveniently implemented in metal insulator metal (MIM) technology, which, compared to interdigital implementations proposed before [2], exhibits the advantages of higher compactness, easier design and immunity to spurious resonances.
The layout of the proposed MIM CRLH antenna unit cell is shown in Fig. 4 along with its parameters. The top and bottom substrates have both a relative permittivity of 7.8 with tan δ of 0.0037 and thicknesses of 0.4 mm and 1.2 mm, respectively.

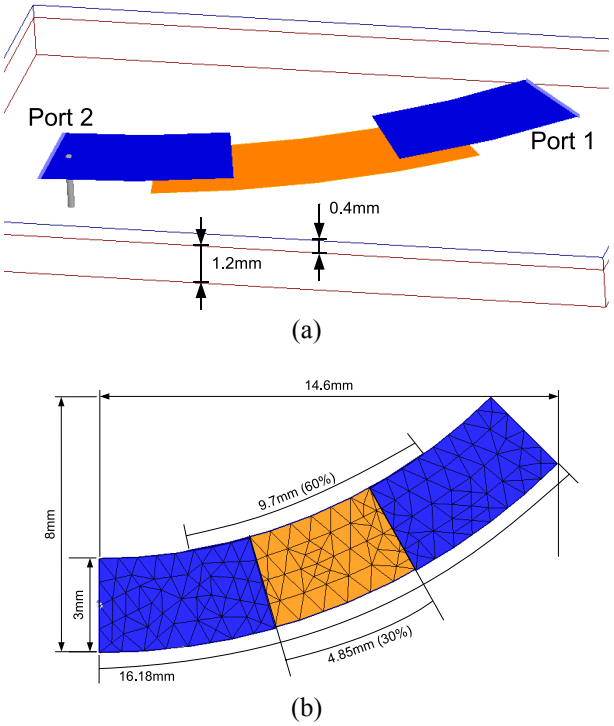

Figure 4. MIM CRLH antenna unit cell (asymmetric) with its parameters. (a) Perspective view. (b) Top view. The inner and outer radii of the ring are 17.6 mm and 20.6 mm, respectively.

4. CRLH PARAMETER EXTRACTION

The parameters of the CRLH unit cell may be quickly extracted from inspection of the full-wave simulated Y and Z parameters, which are shown in Figs. 5, in the following manner. For the asymmetric CRLH unit cell of Fig. 4, we have

$$y_{11}(\omega) = \frac{1}{\mathrm{j}\omega L_{\mathrm{R}} + \dfrac{1}{\mathrm{j}\omega C_{\mathrm{L}}}}. \quad (8)$$

The pole of this expression provides ω_{se} while its derivative at the origin ($\omega \to 0$) provides C_{L}, so that L_{R} is also immediately available. The parameters L_{L} and C_{R} are obtained similarly from

$$z_{22}(\omega) = \frac{1}{\mathrm{j}\omega C_{\mathrm{R}} + \dfrac{1}{\mathrm{j}\omega L_{\mathrm{L}}}}. \quad (9)$$

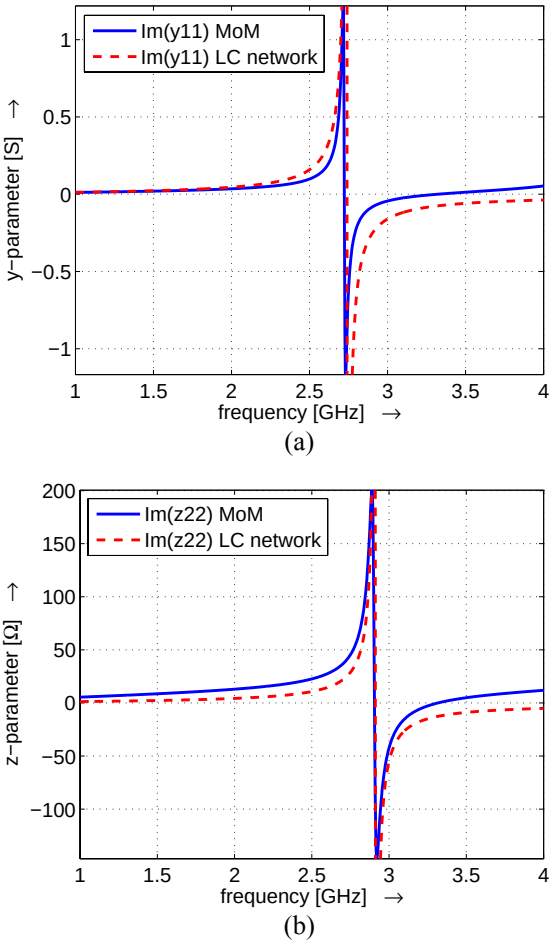

Figure 5. Simulated parameters used for the extraction of the CRLH parameters. (a) $y_{11}(f)$. (b) $z_{22}(f)$.

The parameters for the design of Fig. 4 extracted by this technique with the help of Fig. 5 are C_{R} = 0.17 pF, C_{L} = 1.7 pF, L_{R} = 2 nH, L_{L} = 0.18 nH. The corresponding dispersion diagram with N = 8 is shown in Fig. 6. In this case, the design is not perfectly balanced.

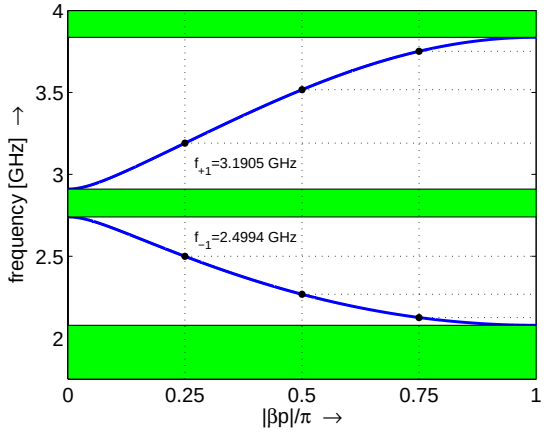

Figure 6. Dispersion diagram and resonances for the design of Fig. 4 with N = 8.

This section has described the extraction of the CRLH parameters, which is an analysis procedure of a given antenna unit cell. In practice, the synthesis of the antenna for a specified pair of frequencies may be carried out by the design procedure given in Sec. 2.

5. FEEDING STRUCTURE

Fig. 7 shows the feeding structure of the antenna. It consists of a microstrip line terminated by a patch (in the plane of the MIM floating patches) capacitively coupled to the upper layer of the ring. The optimized parameters for the dual-band matching are indicated in Fig. 7.

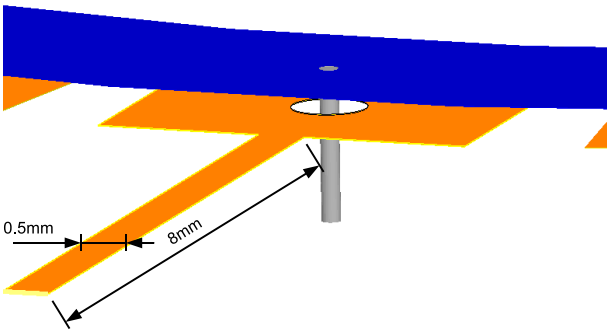

Figure 7. Feeding structure with the following geometrical parameters: line length l_{Feed} = 8 mm, line width w_{Feed} = 0.5 mm, patch dimensions 4×3 mm^2.

6. LINEAR AND CIRCULAR POLARIZATION

The current distribution for both the $n = +1$ and $n = -1$ modes along the ring and ports arrangement for linear and circular polarizations are shown in Fig. 8.

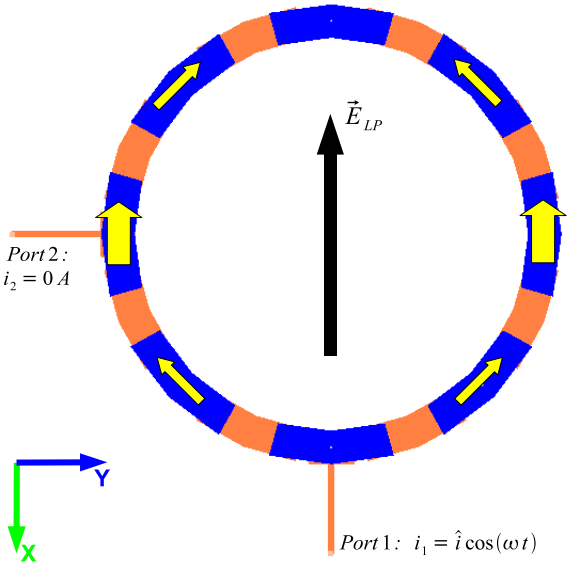

(a)

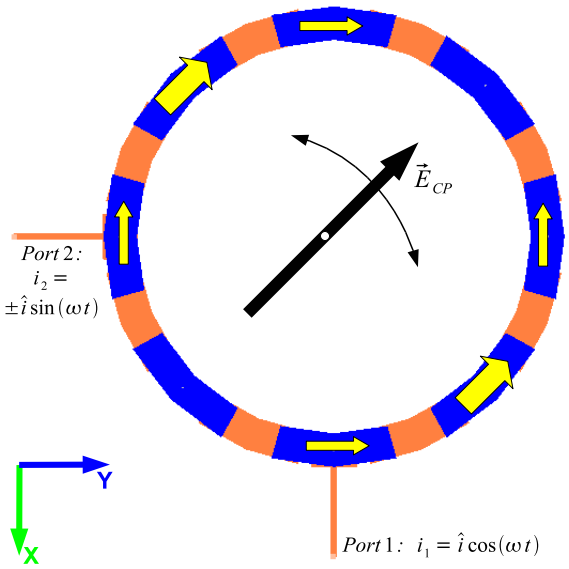

(b)

Figure 8. Current distribution for both the $n = +1$ and $n = -1$ modes along the ring and ports arrangement for linear and circular polarizations.

Depending on the states of the switches in each port, different polarizations are achieved: linear x-directed, linear y-directed, linear xy-directed (both port signals in phase) or circular (both port signals with ±90° phase difference).

7. RESULTS

Fig. 8 shows the two port feeding topology of the antenna. An isolation better than 30 dB is achieved at both operation frequencies f_{-1} and f_{+1}. In the case of single port excitation (with the other one open) for linear polarization, the return loss of both ports is essentially identical since the ports are inherently isolated due to their quadrature relation.

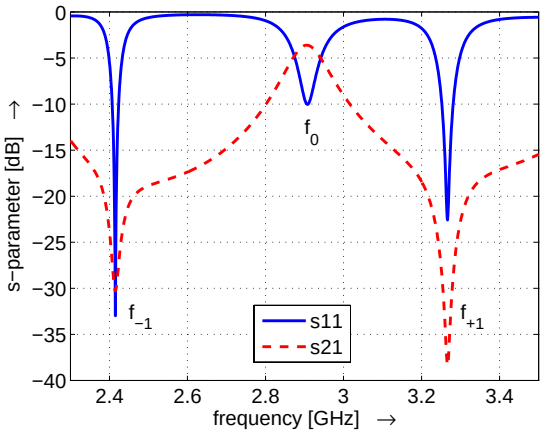

Figure 9. MoM full-wave simulated S-parameter for the two-port antenna.

The radiation pattern of the linearly and circularly polarized antenna are shown in Figs. 10 and 11, respectively. For the linear polarization case, as expected from the larger electrical size of the antenna at the higher frequency, the co-pol gain at this frequency is larger than that of the lower one; on the other hand, the co/cross-pol discrimination of the lower frequency is superior to that of the higher one. For the circular polarization, the radiation patterns for the two modes are qualitatively identical; an excellent co/cross-pol discrimination of 25 dB is observed at broadside direction.

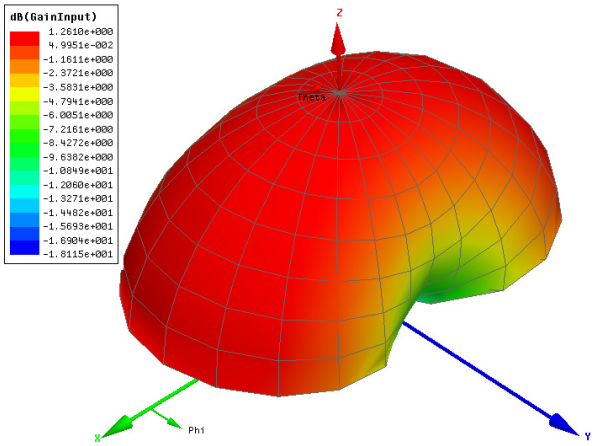

(a)

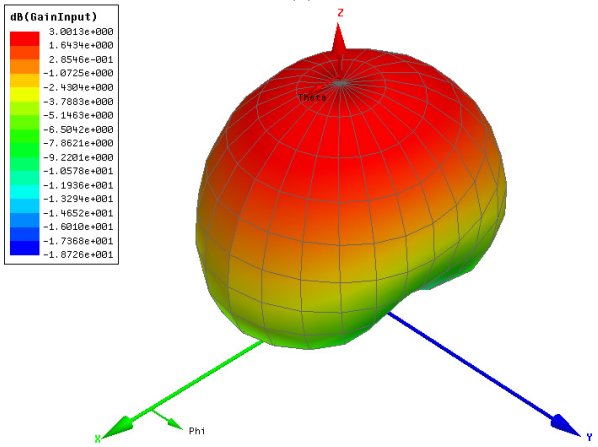

(b)

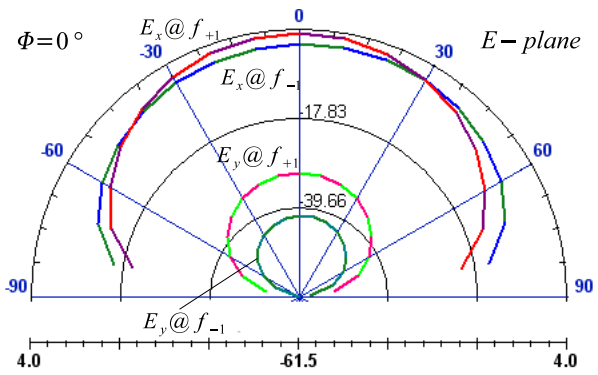

(c)

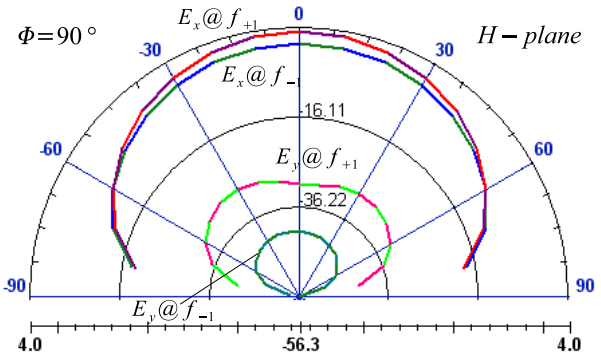

(d)

Figure 10. Radiation pattern for the case of linear polarization (1 port fed). The co-pol input gain is 1.3 dBi for the lower frequency and 3 dBi for the higher frequency.

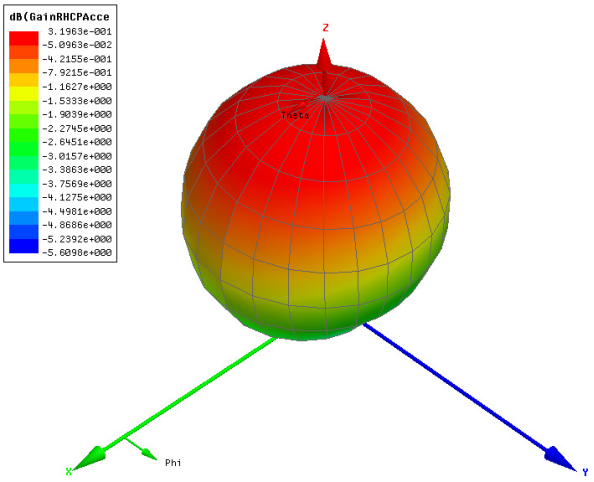

(a)

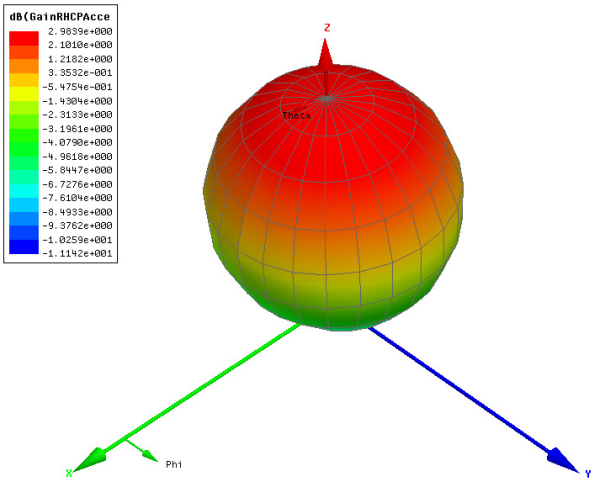

(b)

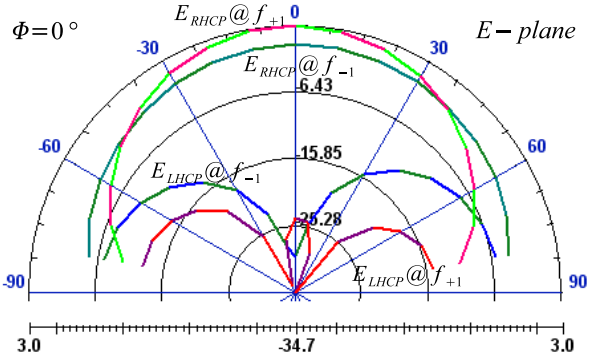

(c)

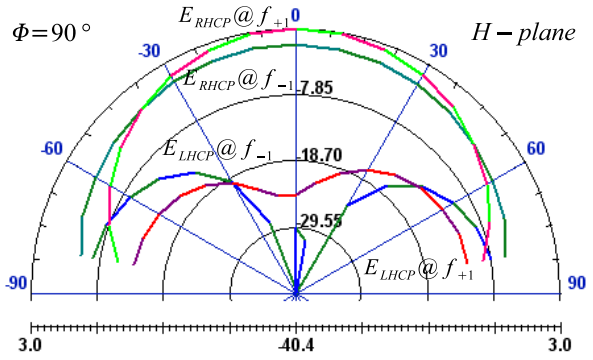

(d)

Figure 11. Radiation pattern for the case of circular polarization (2 ports fed in quadrature). The co-pol CP gain is 0.32 dBi for the lower frequency and 3 dBi for the higher frequency.

8. CONCLUSION

A novel dual-band linear/circular-polarization MIM CRLH ring antenna has been proposed and demonstrated by full-wave simulation. This antenna will be soon implemented in LTCC technology. It may find various applications in wireless LAN and MIMO systems. In [4] the advantages of such a multi-polarization wireless system including the antennas have been discussed.

References

[1] C. Caloz and T. Itoh, *Electromagnetic Metamaterials, Transmission Line Theory and Microwave Applications*, Wiley and IEEE Press, 2005.

[2] S. Otto, A. Rennings, C. Caloz, P. Waldow, and T. Itoh, "Composite right/left-handed λ-resonator ring antenna for dual-frequency operation," in Proc. IEEE AP-S, June 2005, CD-ROM.

[3] H. V. Nguyen and C. Caloz, "Broadband highly selective bandpass filter based on a tapered coupled-resonator (TCR) CRLH structure," Proc. of the European Microwave Association, vol. 2, March 2006.

[4] P. S. Neelakanta and W. Preedalumpabut and S. Morgera, "Making of a robust microwave wireless link: a novel scheme of polarization sense diversity", Microwave Journal, August 2004.